



Scalable population estimates using spatial-stream-network (SSN) models, fish density surveys, and national geospatial database frameworks for streams

Journal:	<i>Canadian Journal of Fisheries and Aquatic Sciences</i>
Manuscript ID	cjfas-2016-0247.R2
Manuscript Type:	Rapid Communication
Date Submitted by the Author:	05-Nov-2016
Complete List of Authors:	Isaak, Daniel; USDA Forest Service Ver Hoef, Jay; National Marine Fisheries Service - NOAA, Alaska Fisheries Science Center Peterson, Erin; Queensland University of Technology Horan, Dona; USDA Forest Service Rocky Mountain Region Nagel, David; USDA Forest Service
Keyword:	spatial-stream network, block-kriging, fish density, population estimate, geostatistics

SCHOLARONE™
Manuscripts

1
2
3
4
5
6
7
8
9
10
11
12
13
14
15
16
17
18

**Scalable population estimates using spatial-stream-network (SSN) models,
fish density surveys, and national geospatial database frameworks for streams**

Daniel J. Isaak^{1*}, Jay M. Ver Hoef², Erin E. Peterson³, Dona L. Horan¹, David E. Nagel¹

¹U.S. Forest Service Rocky Mountain Research Station, Boise ID 83702

²Marine Mammal Laboratory, NOAA-NMFS Alaska Fisheries Science Center, 7600 Sand Point Way NE,
Seattle, WA 98115

³ARC Centre of Excellence for Mathematical and Statistical Frontiers and the Institute for Future
Environments, Queensland University of Technology (QUT), QLD, Australia

*Corresponding author (disaak@fs.fed.us)

19 **Abstract:** Population size estimates for stream fishes are important for conservation and
20 management but sampling costs limit the extent of most estimates to small portions of river
21 networks that encompass 100s–10,000s of linear kilometers. However, the advent of large fish
22 density datasets, spatial-stream-network (SSN) models that benefit from non-independence
23 among samples, and national geospatial database frameworks for streams provide the
24 components to create a broadly scalable approach to population estimation. We demonstrate such
25 an approach with trout density surveys from 108 sites in a 735 kilometer river network.
26 Universal kriging was used to predict a continuous map of densities among survey locations and
27 block kriging (BK) was used to summarize discrete map areas and make population estimates at
28 stream, river, and network scales. The SSN models also accommodate covariates, which
29 facilitates hypothesis testing and provides insights about factors affecting patterns of abundance.
30 The SSN-BK population estimator can be applied using free software and geospatial resources to
31 develop valuable information at low cost from many existing fisheries datasets.
32
33 Keywords: spatial-stream-network, block kriging, fish density, population estimate, geospatial

34 **Introduction**

35 Answering the question “How many fish live in that stream, river, or lake?” is of
36 fundamental importance to fisheries management and species conservation efforts. Estimation
37 methods addressing that question form an extensive literature and many sampling techniques
38 have been developed to collect datasets for use with estimators (Hilborn and Walters 1992; Zale
39 et al. 2013). In lotic systems, fish are often sampled by electrofishing, angling, or snorkeling
40 (Dunham et al. 2009) and population estimates are obtained for short reaches of stream using
41 mark-recapture (Peterson 1896; Lincoln 1930) or depletion-removal estimators (Zippin 1958).
42 For nest-building species like salmon and trout, it is also common to conduct visual surveys
43 during the spawning season and use nest counts as a density index or measure of population size
44 (Al-Chokhachy et al. 2005; Falke et al. 2013). Collectively, those estimates form the core
45 datasets that state and federal management agencies use to monitor the status and trends of many
46 species and fisheries throughout North America and Europe. Thousands of stream and river sites
47 have been sampled in previous decades to estimate local population sizes (Wenger et al. 2011;
48 Meyer et al. 2013; Millar et al. 2016) and as these databases grow, so too do opportunities to
49 mine them for novel information (Isaak et al. 2014).

50 What is considered a “population” when applying traditional estimators to short sections
51 of stream rarely matches the spatial scales at which habitats are occupied by reproducing
52 populations. Most reproducing populations of stream fishes occupy 1s–10s of network
53 kilometers and are affected by natural gradients and anthropogenic stressors occurring over
54 similar scales (Schlosser 1991). The mismatch between measurement scale and biological reality
55 lies at the heart of the Riverscapes paradigm articulated by Fausch et al. (2002) and creates the
56 fundamental need for spatially continuous broad-scale information to better understand and
57 conserve freshwater fishes. Spatial sampling strategies like that espoused by Hankin and Reeves
58 (1988) or more recent attempts (Stevens and Olsen 2004; Torgerson et al. 2006; Korman et al.
59 2016) partially address information needs but are costly and difficult to implement in hundreds
60 of streams throughout the ranges of species or across the 100s–10,000s of linear kilometers that
61 constitute river networks. Another critical and largely unrecognized impediment to developing
62 spatial fisheries information has been the lack of consistent geospatial database frameworks for
63 streams to enable efficient organization, summarization, and sharing of data within or among
64 agencies (Cooter et al. 2010). Such frameworks would provide a database structure wherein each

65 stream reach within a river network is assigned a unique identifier, attributed with topological
66 information (e.g., up- and downstream flow-routing), and georeferenced in a cartographic
67 projection system. Networks with those properties could bridge between relational databases
68 (e.g., Access or Oracle) that are used to store large fisheries datasets and geographic information
69 systems (GIS) that would be used to manipulate and visualize data associated with broadscale
70 population estimation. Also required are flexible analytical tools for data collected from stream
71 networks, especially those capable of accommodating the clustered, non-independent sample
72 locations that inevitably arise during the history of resource agencies or when data are
73 aggregated from multiple sources.

74 In recent years, key statistical and technical advances addressed many of the preceding
75 issues to provide the basic elements for creating a broadly scalable approach to population
76 estimation. The development of spatial-stream-network (SSN) models (Ver Hoef et al. 2006; Ver
77 Hoef and Peterson 2010) based on covariance structures for network topology (Peterson and Ver
78 Hoef 2010) and that rely on assumptions about the stochastic processes generating observable
79 data (Schabenberger and Gotway 2005), facilitates valid inference from non-independent stream
80 samples. As extensions of the linear-mixed model, SSNs accommodate covariates to describe
81 relationships with response variables and simulation studies indicate their accuracy in fixed
82 effect parameter estimation and confidence interval coverage for a wide range of conditions
83 (Som et al. 2014; Rushworth et al. 2015). Concerns have been raised about "spatial confounding"
84 in the estimation of fixed effect parameters (Hodges and Reich (2015) but see Hanks et al.
85 (2015) for a counter-argument) but such confounding is of limited relevance for making accurate
86 spatial predictions. Like other spatial statistical models (Ver Hoef 2002; Beale et al. 2010;
87 Temesgen and Ver Hoef 2015), SSNs consistently improve predictive performance relative to
88 non-spatial models when used with spatially dense datasets that contain non-independent
89 samples (Isaak et al. 2010; Brennan et al. 2016; Turschwell et al. 2016). Classical geostatistical
90 techniques (Cressie 1993) have also been adapted for implementation with the SSN models
91 based on stream distances rather than Euclidean distances, which enables kriging and block-
92 kriging predictions to be made throughout river networks with spatially explicit errors (Ver Hoef
93 et al. 2006).

94 Paralleling the development of SSN models has been the development of nationally
95 consistent geospatial frameworks for stream data (Cooter et al. 2010; Moore and Dewald 2016).

96 Most notably for Canada, lotic systems are represented by the National Hydro Network (NHN;
97 http://ftp2.cits.rncan.gc.ca/pub/geobase/official/nhn_rhn/doc/NHN.pdf), and within the United
98 States by the National Hydrography Dataset (NHD; [www.horizon-](http://www.horizon-systems.com/NHDPlus/NHDPlusV2_home.php)
99 [systems.com/NHDPlus/NHDPlusV2_home.php](http://www.horizon-systems.com/NHDPlus/NHDPlusV2_home.php)). The NHD is available in several resolutions,
100 but of particular value is the medium resolution version (1:100,000-scale) because of the reach
101 descriptor variables (e.g., elevation, slope, watershed size, and many others) that have been
102 incorporated as Value Added Attributes to create NHDPlus (McKay et al. 2012). The reach
103 descriptors can be used to query stream networks, visualize results within a GIS, and as
104 covariates in predictive models. As the user-community associated with NHDPlus has grown,
105 dozens of additional reach descriptors have been developed by groups like the National Fish
106 Habitat Partnership (Wang et al. 2011) and the Environmental Protection Agency (Hill et al.
107 2016).

108 In this paper, we integrate SSN models and the geospatial resources described above with
109 a fish density dataset to develop a scalable approach to population estimation. Models that
110 predict fish density are developed based on different combinations of covariates and
111 autocovariance functions that account for non-independence among samples. The models are
112 used to predict continuous density maps, which are then summarized to make population
113 estimates at stream, river, and network scales. For comparison to non-spatial analogues,
114 estimates are also made using multiple linear regression (MLR) and simple random sampling
115 (SRS). The dataset and statistical code used in the analysis are included as supplemental
116 materials so that interested readers may explore these topics in detail.

117

118 **Materials and methods**

119 **Study area and dataset**

120 A dataset of trout density estimates at 108 sites was obtained from the 2,300 km² Salt
121 River watershed on the border between Idaho and Wyoming in the western U.S. The area is
122 mountainous and 11 major tributaries drain north-south trending ranges at the eastern and
123 western extents of the watershed (Figure 1). Tributaries and several spring streams that originate
124 from the main valley floor were sampled at 104 locations during summer low-flow conditions
125 (stream widths: 1.2–8.8 m, reach lengths: 63–465 m) in 1996 and 1997 by electrofishing within
126 block-netted reaches to obtain local population estimates for age-1+ trout using depletion

127 methods (Zippin 1958; Isaak and Hubert 2004). Samples were spaced at 50-m elevation intervals
128 along most tributaries with additional samples taken near tributary confluences or upstream and
129 downstream of abrupt contrasts in channel slope. Those data were supplemented with population
130 estimates from four sites on the Salt River mainstem (river widths: 20 – 32 m, reach lengths:
131 4.4–4.8 km) that were repeated in 1995, 1996, and 1998 by raft electrofishing using mark-
132 recapture methods (Pollock et al. 1990; Gelwicks et al. 2002). For current purposes, the Salt
133 River estimates were averaged across years. Species composition, based on approximately 5,000
134 trout captured at the 108 sites, was 82.6% native Yellowstone cutthroat trout (*Oncorhynchus*
135 *clarkii bouvieri*), 12.7% non-native brown trout (*Salmo trutta*), 4.6% non-native brook trout
136 (*Salvelinus fontinalis*), and 0.1% non-native rainbow trout (*O. mykiss*). Population estimates at
137 the 108 sites were standardized as trout•100 m⁻¹ length of stream. Additional details about the
138 dataset and study area are provided elsewhere (Gelwicks et al. 2002; Isaak and Hubert 2004).

139 A digital stream network for the NHD processing unit (Pacific Northwest 17) that
140 encompassed the Salt River watershed was downloaded from the National Stream Internet
141 website (NSI; www.fs.fed.us/rm/boise/AWAE/projects/NationalStreamInternet.html; Isaak et al.
142 2013) and clipped using the watershed boundary. The NSI network is derived from the
143 1:100,000-scale NHDPlus Version 2 network, has been topologically adjusted to facilitate SSN
144 analysis using the Spatial Tools for the Analysis of River Systems software (STARS; Peterson
145 and Ver Hoef 2014), and is available for all streams and rivers in the coterminous U.S. A one-to-
146 one relationship between reaches in the NSI and NHDPlus networks facilitates the use of NHD
147 reach descriptors as covariates in SSN models. Here, we considered only a small number of
148 covariates (reach slope, summer temperature, and stream canopy density), which have previously
149 been associated with trout densities (Chisholm and Hubert 1986; Fausch et al. 1988; Isaak and
150 Hubert 2004) and were available as reach descriptors in geospatial formats (Table 1). The NHD
151 and NSI networks contain many reaches that do not support fish populations because of
152 intermittent flow or excessive steepness, so the original Salt River network of 1,901 km was
153 trimmed to a 735-km network prior to analysis by deleting reaches with >10% slope, those coded
154 as intermittent in the NHDPlus dataset (e.g., Fcode = 46003), and based on observations made by
155 the lead author during field sampling. We processed the final dataset using the current version of
156 STARS (Peterson and Ver Hoef 2014, Version 2.0.4 downloaded from the SSN/STARS website:
157 www.fs.fed.us/rm/boise/AWAE/projects/SpatialStreamNetworks.shtml) and output the spatial,

158 topological, and attribute information as a Landscape Network object (LSN; available as
 159 Supplemental A) suitable for spatial analysis. The SSN package (Ver Hoef et al. 2014; Version
 160 1.1.7) for the R statistical software (R Development Core Team 2014) was downloaded from the
 161 Comprehensive R Archive Network website (www.r-project.org/) and used with the LSN object
 162 to conduct all subsequent analyses.

163 To describe spatial similarity, often referred to as autocorrelation, in the trout density
 164 dataset, a type of semivariogram called a Torgegram was initially calculated (Zimmerman and
 165 Ver Hoef 2017). The semivariance is one-half of the average squared difference between random
 166 variables separated by some intervening distance (Matheron 1963). If s_i and s_j contain the spatial
 167 coordinates for the i th and j th locations, and $y(s_i)$ and $y(s_j)$ are the measured values at those
 168 locations, then an empirical estimator of the semivariance, $\gamma(h)$, is

$$(1) \quad \gamma(h) = \frac{1}{2N(h)} \sum_{\|s_i - s_j\| \in c(h)} [y(s_i) - y(s_j)]^2,$$

169 where h is the distance, $\|s_i - s_j\|$, between locations, $c(h)$ is the distance bin representing the
 170 interval around h (chosen to be mutually exclusive and exhaustive so that all distances h fall into
 171 one of the bins), and $N(h)$ is the number of data pairs (s_i, s_j) in distance bin $c(h)$. The
 172 semivariogram provides a graphical representation of spatial autocorrelation in the measured
 173 data; when semivariance values are low (high) it indicates that sample pairs within a distance bin
 174 are similar (dissimilar). If positive autocorrelation occurs within a dataset, the semivariance
 175 values are smallest at short distance lags and increase as distance increases. The Torgegram is
 176 similar to a traditional semivariogram except that semivariance values are plotted separately for
 177 site-pairs with flow-connected (e.g. water flows from an upstream site through a downstream
 178 site) and flow-unconnected (e.g. sites reside on the same network but do not share the same flow)
 179 relationships because these patterns usually differ on stream networks (Peterson et al. 2013;
 180 Zimmerman and Ver Hoef 2017). As expected, given the density of the trout samples, the
 181 Torgegram showed strong similarities among site estimates in close proximity and weaker
 182 similarities as separation distances increased (Figure 2). Semivariance among flow-unconnected
 183 sites plateaued at approximately 10 km while semivariance among flow-connected sites steadily
 184 increased to the maximum distance of 50 km. Those patterns indicated that trout densities
 185 became dissimilar among adjacent headwater streams (i.e., flow-unconnected relationships) over

186 shorter geographic distances than did densities along flow-connected pathways from headwaters
187 to the river mainstem.

188

189 **SSN trout density models**

190 Five SSN models were fit to the trout density dataset in R using the SSN package (a copy
191 of the R script is provided as Supplemental B). Three of those models included reach covariates
192 and two models used only an intercept (i.e., mean trout density) with an autocovariance function
193 (Table 2), which was equivalent to ordinary kriging. In all cases, the basic linear mixed model
194 we used was

$$(2) \quad \mathbf{y} = \mathbf{X}\boldsymbol{\beta} + \mathbf{z}_{\text{TU}} + \mathbf{z}_{\text{TD}} + \mathbf{z}_{\text{EUC}} + \boldsymbol{\varepsilon},$$

195 where \mathbf{y} is a vector of measured trout densities, \mathbf{X} is a matrix of covariate values, $\boldsymbol{\beta}$ is a vector of
196 regression coefficients, and $\boldsymbol{\varepsilon}$ is a vector of independent and normally distributed random errors.
197 The spatial structure in residuals was described using vectors of zero-mean random variables
198 (\mathbf{z}_{TU} , \mathbf{z}_{TD} , and \mathbf{z}_{EUC}) with a autocorrelation structure based on tail-up (TU), tail-down (TD), and
199 Euclidean (EUC) covariance functions (Peterson and Ver Hoef 2010, Ver Hoef and Peterson
200 2010). Each random variable (\mathbf{z}_{TU} , \mathbf{z}_{TD} , \mathbf{z}_{EUC}) in the autocorrelation structure can be represented
201 by one of several different covariance models (e.g., linear-with-sill, Mariah, exponential,
202 Epanechnikov, spherical models; Chiles and Delfiner 2009, Garreta et al. 2010). Moreover, one
203 or more classes of covariance function (TU, TD, EUC) may be chosen to represent the properties
204 of the stream attribute being modeled (e.g. patterns created by passive downstream diffusion or
205 upstream and downstream movement processes). The choice of covariance function(s) is
206 important because each represents spatial relationships in a different way. The tail-up function
207 restricts correlation to sites that are flow-connected and uses spatial weighting based on user-
208 specified stream attributes (e.g., watershed area, stream order, segment slope) to up- or down-
209 weight samples that occur upstream of a location (Frieden et al. 2014). The tail-down function, in
210 contrast, permits correlation between both flow-connected and flow-unconnected locations and a
211 spatial weighting scheme is not necessary. For simplicity, we drew on previous results that
212 suggest a mixed covariance construction usually performs best (Peterson and Ver Hoef 2010;
213 Frieden et al. 2014) and used exponential models for the TD, EUC, and TU functions, with the
214 TU weighting scheme based on watershed area.

215 The five SSN models were compared using the Akaike Information Criterion (AIC,
 216 Akaike 1974), penalizing for the number of covariate and autocovariance parameters. Leave-
 217 one-out cross-validation (LOOCV) was used to assess the predictive performance of models in
 218 two ways. We computed r^2 for a linear model that related LOOCV predictions to observed trout
 219 densities, and we computed the root mean square prediction error as

$$(3) \quad RMSPE = \sqrt{\frac{\sum_{i=1}^n [\hat{y}(s_i) - y(s_i)]^2}{n}},$$

220 where $y(s_i)$ is the observation at location s_i , $\hat{y}(s_i)$ is the LOOCV prediction value for s_i , and n is
 221 the total number of observed data values. Maximum likelihood (ML) estimation was used for
 222 parameter estimation so that AIC values were valid for model comparisons but restricted
 223 maximum likelihood (REML) was used for all other estimation purposes (Ver Hoef et al. 2014).
 224 As a baseline for comparison with the SSN models, we also fit a non-spatial MLR model to the
 225 trout density dataset, which was based on the assumption that residual errors were spatially
 226 independent. The same set of performance metrics was also calculated for the MLR model.

227

228 **Block-kriging population estimates**

229 The SSN models were used to predict trout densities at 100 m intervals throughout the
 230 Salt River network using universal kriging (Cressie 1993). The kriging equations have two parts,
 231 predictions based on the linear regression model and adjustments based on local spatial
 232 autocorrelation,

$$(4) \quad \hat{y}(s_0) = \mathbf{x}(s_0)' \hat{\boldsymbol{\beta}} + \mathbf{c}(s_0)' \boldsymbol{\Sigma}^{-1} (\mathbf{y} - \mathbf{X} \hat{\boldsymbol{\beta}}),$$

233 where $\mathbf{x}(s_0)$ is a vector containing the covariate values at prediction location s_0 and the vector $\hat{\boldsymbol{\beta}}$
 234 contains the estimated regression coefficients using REML, so $\mathbf{x}(s_0)' \hat{\boldsymbol{\beta}}$ forms the linear
 235 regression prediction. The remaining portion of equation 4 is an adjustment for spatial
 236 autocorrelation, where $\mathbf{c}(s_0)$ is a vector of covariances among observed data and the prediction
 237 site, and $\boldsymbol{\Sigma}$ is the covariance matrix among observed data. This kriging formulation provides
 238 exact interpolations that "honor the data" in contrast to alternatives based on splines
 239 (Schabenberger and Gotway 2005). Local prediction variances (Ver Hoef 2008) are given by

$$(5) \quad \hat{\text{var}}[\hat{y}(s_0)] = \sigma_0^2 - \mathbf{c}(s_0)' \boldsymbol{\Sigma}^{-1} \mathbf{c}(s_0) + \mathbf{d}' (\mathbf{X}' \boldsymbol{\Sigma}^{-1} \mathbf{X})^{-1} \mathbf{d},$$

240 where $\sigma_0^2 = \text{var}[y(s_0)]$ (including all of the variance components) and $\mathbf{d} = \mathbf{x}(s_0)' -$
241 $\mathbf{X}'\boldsymbol{\Sigma}^{-1}\mathbf{c}(s_0)$.

242 Population estimates were developed from the network predictions using block kriging
243 (BK), which predicts an average value from an integral of a random surface. The mean integral
244 for a portion of a stream network, B_0 , is

$$(6) \quad \hat{y}(B_0) = \frac{1}{b-a} \int_a^b y(u) du$$

245 If the integral is over a stream network, then integrals are done piece-wise for each stream
246 segment, added together, and then divided by the total length of integrated stream. In practice,
247 the integral is approximated using a grid of evenly-spaced prediction points along the network.
248 Block-kriging predictions and variances require modification of equations 4 and 5 wherein $\mathbf{c}(s_0)$
249 is replaced by $\mathbf{c}(B_0)$ and all pairwise covariances are computed between the observed data and
250 the points on the grid used to approximate an integral. Similar modifications are required for σ_0^2
251 in equation 5, and covariates need to be integrated as well. The necessary two-dimensional
252 formulas are given in Ver Hoef (2008), have been adapted for streams (Ver Hoef et al. 2006),
253 and the functionality is included in the SSN package so that BK predictions and variances can be
254 easily generated by users (Ver Hoef et al. 2014).

255 To approximate the integrals for population estimates in the Salt River network, we
256 created a grid of points at 100 m intervals throughout the network. The BK estimate of trout
257 density over any network subset then yielded an estimate of the mean trout density, so the
258 population estimate was this density times the length of the network subset. Figure 1 shows the
259 locations where population estimates were made in tributaries and the Salt River mainstem. The
260 same BK procedure was conducted for the full network that supported fish populations to obtain
261 a grand population estimate for the watershed. When making the grand estimate, we excluded
262 downstream sections of some tributaries that are dewatered for irrigation purposes during the
263 summer. As a baseline for comparison, we also derived population estimates for the same areas
264 using a non-spatial SRS estimator with the observed densities (as in classical design-based
265 surveys (Thompson 1992)), which were then expanded based on appropriate stream-length
266 factors.

267

268 Results

269 Trout densities at the 108 sites ranged from 0 to 132 trout•100 m⁻¹ and showed
270 geographic clustering of similar densities (Figure 1) that corroborated the Torgegram results
271 (Figure 2). Densities were usually lowest in the highest elevation stream sites along the eastern
272 portion of the watershed and higher in most western tributaries and the Salt River mainstem. The
273 five SSN models had similar predictive accuracies (LOOCV $r^2 \sim 0.49$; RMSPE ~ 21.0) and
274 showed considerable performance gains relative to the MLR (LOOCV $r^2 = 0.19$; RMSPE = 26.3;
275 Table 2). Both types of models overestimated low densities and underestimated high densities
276 but the SSN models did so to a lesser degree (Figure 3). The SSN models had AIC scores that
277 were 20–27 points lower than the MLR, despite requiring the estimation of 2–7 additional
278 parameters for the autocovariance functions (Table 2). The temperature covariate was
279 statistically significant in the models where it appeared ($p < 0.05$) and reach slope was never
280 significant. The canopy covariate was significant in the MLR ($p = 0.02$) but not in the SSNs ($p \geq$
281 0.14). Within the SSN model set, SSN3 that used a temperature covariate and TU, TD
282 autocovariance function had the lowest AIC value. Two models without covariates (SSN4 and
283 SSN5) has similar predictive performance as SSN3 but had AIC scores 5–7 points higher. A
284 trout density map predicted using SSN3 showed how abundance varied throughout the network
285 (Figure 4). Noteworthy was that predictions matched observed densities at the 108 sample sites,
286 which is a property of the kriging formulation that was implemented. Also noteworthy was the
287 spatial variation in the size of the prediction standard errors, which were smaller near sample
288 sites because the SSN model used the fitted autocovariance function and local empirical support
289 when making predictions.

290 Population estimates based on SRS and the five SSN models showed several interesting
291 properties when examined for four representative tributaries (Figure 5). First, SSN-BK estimates
292 could be made for all streams, which was not the case with the SRS estimator in Swift Creek
293 where only one density sample was available (two samples are needed to calculate a variance
294 and confidence interval). Second, results from Willow Creek support the notion that SSN-BK
295 estimates may often be more accurate than those from SRS. Five density samples were available
296 in that stream but only one occurred in the downstream segment where trout densities were high,
297 so the SRS population estimate of ~4,000 trout was biased low compared to the BK estimate of
298 ~7,000 trout made from a spatially balanced set of predictions throughout the stream. Third,

299 SSN-BK estimates for individual streams were similar regardless of the model chosen, which
300 suggested robustness to different specifications.

301 A full set of SRS and SSN3-BK population estimates for streams in the Salt River
302 network is provided in Figure 6. The SSN3-BK estimates were usually more precise and showed
303 that eastern tributaries had smaller trout populations (612–7,128 trout) than western tributaries
304 (12,963–27,216 trout) and the Salt River mainstem (42,987 +/-11,894 trout (95% CI)). The
305 difference in population estimates was primarily due to the shorter networks that comprised
306 eastern tributaries, but those streams were also especially cold and may have been too
307 unproductive to support high trout densities as indicated by the positive effect of the temperature
308 covariate in the SSN models. The grand SSN3-BK population estimate for the Salt River
309 network was 184,030 +/-27,263 trout; whereas the SRS estimate was 155,828 +/- 26,514 trout.
310 Similar to the bias associated with the Willow Creek estimate, the SRS estimate for the full
311 network may have been biased by the large proportion of samples from high elevation tributaries
312 where trout densities were lower (Figure 1). That bias could have been addressed using a
313 stratified random sampling estimator wherein each tributary was treated as a stratum but single
314 samples from some strata would have made variance calculations impossible without ad hoc
315 combinations of multiple streams into workable strata.

316

317 **Discussion**

318 Combining fish density surveys and SSN models with broadly available geospatial data
319 frameworks creates a powerful and flexible approach to population estimation for streams and
320 rivers. As we demonstrate, population estimates can be derived at virtually any spatial scale,
321 thereby allowing biological information to be matched with relevant land-uses, landscape
322 features, or jurisdictional and biogeographic boundaries to address conservation and
323 management needs. For example, population estimates at stream or network scales are key for
324 species' conservation assessments (e.g., the 50/500 rule, Franklin 1980), but have rarely been
325 available or are based on extrapolations from a small number of non-random samples
326 (Hilderbrand and Kershner 2000; Cook et al. 2010). Estimates like those developed here for the
327 Salt River basin, which hosted ~150,000 of the native Yellowstone cutthroat trout (a species of
328 conservation concern), can now be repeated elsewhere to inform status assessments where
329 sufficient data exist. Although 50–100 samples are desirable to estimate parameters for the SSN

330 models (Isaak et al. 2014), datasets of this size are common within research and management
331 agencies, especially when data are aggregated across multiple projects or agencies. One example,
332 the MARIS database (Multistate Aquatic Resources Information System: www.marisdata.org;
333 Loftus and Beard 2009), contains >1,000,000 fisheries surveys for >1,000 species in the eastern
334 U.S., an impressive total that nonetheless represents a small fraction of extant data. Another
335 potential application of the SSN-BK estimator was presented by the dewatered stream reaches in
336 the Salt River network, where estimates could have been made for the number of trout those
337 areas would support if perennial flows were restored. Block kriging also has obvious utility for
338 making reference site comparisons used in biological and habitat condition assessments
339 (Kershner and Roper 2010; Hawkins et al. 2010) or within the regulatory arena to determine
340 where standards are exceeded if SSN models are applied to water chemistry attributes (Birkeland
341 2001).

342 A key difference between SSN-BK and previous estimators (e.g., Hankin and Reeves
343 1988; Stevens and Olsen 2004) is that the SSN estimator relies on model-based inference and
344 does not require random sampling (Ver Hoef 2008). Even when designs are randomized, better
345 estimates are often possible using spatial models because random designs have some degree of
346 clustering and ancillary spatial information exists that is useful for estimation (Ver Hoef 2002).
347 The SRS and MLR estimators used in our examples were unweighted, so clustered trout density
348 samples over-represented conditions in some areas and biased results due to spatial unbalance.
349 Although it would have been possible to weight samples in an ad hoc fashion, block-kriging
350 finds an optimal weighting scheme within the blocking area. The SSN-BK estimator is accurate,
351 therefore, because it replaces the average of the observations with an average from an evenly-
352 spaced grid of model predictions that achieves spatial balance. Each prediction is simply a
353 weighted average that has optimality properties, in the sense that it minimizes the mean-squared
354 prediction error (Ver Hoef 2008).

355 Another important feature of the SSN models is their ability to incorporate covariates and
356 assess effect sizes and statistical significance in the presence of spatial autocorrelation. Although
357 the inclusion of covariates in our Salt River dataset provided only small model improvements,
358 developing fully descriptive density models here was not our goal. Those models are a logical
359 next step, however, and one that will be enhanced by the availability of dozens of reach
360 descriptors for the NHD and NSI networks (Wang et al. 2011; Hill et al. 2016) and the increasing

361 technical proficiency of users in developing custom covariates (Peterson et al. 2011; Nagel et al.
362 2014). But as our results also demonstrate, informative covariates are not prerequisite to
363 developing accurate prediction maps with SSN models if datasets are spatially dense and
364 samples are autocorrelated. Those maps can provide detailed information about patterns of
365 abundance and help identify fish density hotspots, which could be useful for directing
366 conservation efforts even without a complete understanding of the processes that create spatial
367 patterns. In the Salt River watershed, for example, the data visualization provided by the
368 prediction maps added considerable depth to our view of the landscape despite a previous
369 familiarity with it. Moreover, the depiction of spatial variation in SSN model prediction
370 precision could be used to guide subsequent sampling efforts to locations that reduced the
371 greatest amount of uncertainty. The Torgegram description of spatial autocorrelation among trout
372 densities might also be useful for designing sampling campaigns in other networks that lack data
373 by providing a first approximation of the stream distances over which samples are partially
374 redundant (Som et al. 2014; Zimmerman and Ver Hoef 2017).

375 There are three caveats regarding the use of the SSN-BK estimator. First, population
376 estimates for headwater streams will be sensitive to errors associated with the length of stream
377 estimated to support fish, which may be problematic in that headwater reaches are often
378 imprecisely mapped (Bishop et al. 2008). Our familiarity with the Salt River study site allowed
379 us to trim the network based on field observations so that it closely approximated fish habitat,
380 but the size of this reduction was substantial (61%) and would have inflated population estimates
381 if not addressed. For applications where investigators lack direct knowledge of local conditions,
382 rulesets to trim the network based on defensible criteria should be developed and applied. Two
383 obvious criteria when using the NHDPlus dataset are intermittency and stream slope. In the latter
384 case, fish densities are low in steep reaches (Chisholm and Hubert 1986; Isaak et al. 2017) so
385 exclusion of these areas in mountain landscapes has minor effects on population estimates. In
386 arid landscapes like much of the American West, the network extent shown by NHDPlus is often
387 far more extensive than the actual length of perennial streams, let alone those large enough to
388 support fish populations (Fritz et al. 2013). Intermittent reaches are coded in NHDPlus (McKay
389 et al. 2012), albeit inconsistently in different river basins, so may sometimes be identified and
390 excluded from analysis. A second caveat pertains to preferential sampling and the possibility that
391 strongly clustered sample locations could bias SSN model estimates (Diggle et al. 2010).

392 Simulation results suggest SSN models perform well with many non-random samples (Falk et al.
393 2014; Som et al. 2014; Rushworth et al. 2015), but practitioners should always be cautious with
394 ad hoc databases and avoid situations where models are fit to geographically restricted data and
395 then extrapolated across a much larger network extent. In addition to clustered samples, it is
396 desirable to have some sample sites spread throughout the network to encompass a broad range
397 of environmental conditions and ensure that parameter estimates and kriging predictions are
398 robust (Courbois et al. 2008; Elith and Leathwick 2009). The third caveat associated with the
399 SSN-BK estimator is that any systematic bias in local population estimates will translate to
400 broad-scale estimates, and the depletion estimator commonly used in small streams is negatively
401 biased (Cook et al. 2010; Meyer and High 2011). That bias could be remedied by using mark-
402 recapture techniques, conducting more electrofishing passes, incorporating detection efficiencies,
403 or applying post-hoc corrections (Peterson et al. 2004; Cook et al. 2010). Accurate local density
404 estimates are desirable but increasing accuracy also comes at a cost when it requires longer
405 sampling durations at individual sites (e.g., mark-recapture estimates). However, if the greatest
406 uncertainty in a broad-scale population estimate stems from sampling a small proportion of the
407 total area, then sampling more sites less accurately could be optimal. That is especially true if the
408 decrease in local accuracy is small, as is often the case with removal estimators because the
409 number of fish captured during the first pass correlates strongly with final estimates based on
410 multiple passes (Cook et al. 2010; Meyer and High 2011). Similar tradeoffs are what ultimately
411 motivated the systematic, broad-scale sampling approach of Hankin and Reeves (1988) and a re-
412 examination of this issue using the spatial statistical simulation capabilities provided in SSN
413 software would be timely (Ver Hoef et al. 2014).

414 Spatial-stream-network models are powerful tools for stream scientists but the recency of
415 their development also means that work remains to develop additional statistical theory and
416 software that broadens their application. Most relevant to abundance estimation would be SSN
417 models that incorporate habitat-related detection efficiencies (Peterson et al. 2004). However,
418 application of those models, or any others, to large datasets aggregated from many sources face
419 challenges associated with inconsistent field habitat measurement protocols (Millar et al. 2016).
420 Standardization of protocols is needed but geospatial representations of habitat conditions that
421 affect detection efficiency (e.g. stream size, reach slope, habitat complexity) may also be an
422 effective alternative that could be implemented consistently across large areas as stream

423 covariate databases and remote sensing applications continue to grow (Carbonneau et al. 2012;
424 Hill et al. 2016). Space-time models are another logical extension of SSN models because repeat
425 sampling of sites is fundamental to many fisheries monitoring programs (Thorson et al. 2015).
426 Geostatistical space-time models have been developed for non-network systems (Cressie and
427 Wikle 2011) but their adaption to streams with appropriate covariance structures is a nontrivial
428 task that requires additional research.

429 We are not the first to recognize the potential benefits of geostatistical methods for
430 stream and river data (Ganio et al. 2005; Durance et al. 2006), nor is this the first attempt to use
431 geospatial technologies to derive population estimates at broader scales (Wyatt 2003; Webster et
432 al. 2008). Only recently, however, has the statistical theory for stream networks developed
433 sufficiently (Peterson et al. 2010; Ver Hoef et al. 2010) and been integrated into robust software
434 (Peterson and Ver Hoef 2014; Ver Hoef et al. 2014) to make the methods broadly accessible to
435 users. The timing is opportune given the increasing availability of large, spatially dense fisheries
436 datasets and geospatial frameworks for organizing data (Cooter et al. 2010; McKay et al. 2012).
437 Developing initial SSN-BK population estimates may require a few weeks of work by those with
438 complementary GIS and statistical skills but it then is possible to derive population estimates at
439 any scale within the modeling domain and to later refine population estimates with additional
440 data. The insights yielded by these new spatial analyses regarding the distribution and abundance
441 of stream fishes should prove useful in addressing many conservation and management issues.

442

443 **Acknowledgements**

444 We thank the Wyoming Game and Fish Department for funding field data collection efforts. M.
445 Hyatt and L. Isaak provided assistance with sampling trout populations in tributary streams. K.
446 Gelwicks and D. Zafft provided trout density data from the Salt River mainstem. D. Isaak was
447 supported by the U.S. Forest Service, Rocky Mountain Research Station during manuscript
448 preparation. Kevin Meyer and three anonymous reviewers provided comments that improved the
449 quality of the final manuscript.

450

451 **References**

- 452 Akaike, H. 1974. A new look at the statistical model identification. IEEE Trans Automat
453 Control. **19**(6):716–722. doi: 10.1109/TAC.1974.1100705.
- 454 Al-Chokhachy, R., Budy, P., and Schaller, H. 2005. Understanding the significance of redd
455 counts: a comparison between two methods for estimating the abundance of and monitoring
456 bull trout populations. N. Am. J. Fish. Manage. **25**(4):1505-1512. doi: 10.1577/M05-006.1.
- 457 Beale, C.M., Lennon, J.J., Yearsley, J.M., Brewer, M.J., and Elston, D.A. 2010. Regression
458 analysis of spatial data. Ecol. Lett. **13**(2):246–264. doi: 10.1111/j.1461-0248.2009.01422.x.
- 459 Birkeland, S. 2001. EPA’s TMDL program. Ecol Law Q **28**(2):297–325. doi:
460 [10.15779/Z38F85M](https://doi.org/10.15779/Z38F85M).
- 461 Bishop, K., Buffam, I., Erlandsson, M., Fölster, J., Laudon, H., Seibert, J., and Temnerud, J.
462 2008. *Aqua Incognita*: the unknown headwaters. Hydrol. Proc. **22**(8):1239-1242. doi:
463 10.1002/hyp.7049.
- 464 Brennan, S.R., Torgersen, C.E., Hollenbeck, J.P., Fernandez, D.P., Jensen, C.K., and Schindler,
465 D.E. 2016. Dendritic network models improve isoscapes and quantify influence of landscape
466 and in-stream processes on strontium isotopes in rivers. Geophys. Res. Lett. **43**(10):5043-
467 5051. doi: 10.1002/2016GL068904.
- 468 Carbonneau, P., Fonstad, M.A., Marcus, W.A. and Dugdale, S.J. 2012. Making riverscapes real.
469 Geomorphology **137**(1):74-86. doi.org/10.1016/j.geomorph.2010.09.030.
- 470 Chiles, J.P., and Delfiner, P. 2009. Geostatistics: Modeling Spatial Uncertainty. John Wiley and
471 Sons.
- 472 Chisholm, I.M., and Hubert, W.A. 1986. Influence of stream gradient on standing stock of brook
473 trout in the Snowy Range, Wyoming. Northwest Science **60**(2):137-139.
- 474 Cook, N., Rahel, F.J., and Hubert, W.A. 2010. Persistence of Colorado River Cutthroat Trout
475 populations in isolated headwater streams of Wyoming. Trans. Am. Fish. Soc. **139**(5):1500–
476 1510. doi: 10.1577/T09-133.1.
- 477 Cooter, W., Rineer, J., and Bergenroth, B. 2010. A nationally consistent NHDPlus framework for
478 identifying interstate waters: implications for integrated assessments and interjurisdictional
479 TMDLs. Environ. Manage. **46**(3):510–524. doi: 10.1007/s00267-010-9526-y.
- 480 Courbois, J.Y., Katz, S.L., Isaak, D.J., Steel, E.A., Thurow, R.F., Wargo-Rub, A.M., Olsen, T.,
481 Jordan, C.E. 2008. Evaluating probability sampling strategies for estimating redd counts: an

- 482 example with Chinook salmon (*Oncorhynchus tshawytscha*). Canadian Journal of Fisheries
483 and Aquatic Sciences. **65**(9):1814-30. doi: 10.1139/F08-092.
- 484 Cressie, N. 1993. Statistics for Spatial Data, Revised Edition. New York: John Wiley and Sons.
485 Cressie, N., and Wikle, C.K. 2011. Statistics for spatio-temporal data. John Wiley and Sons.
486 Hoboken, New Jersey. 588p.
- 487 Diggle, P.J., Menezes, R., Su, T.L. 2010. Geostatistical inference under preferential sampling.
488 Journal of the Royal Statistical Society: Series C (Applied Statistics) **59**(2):191-232. doi:
489 10.1111/j.1467-9876.2009.00701.x.
- 490 Dunham, J.B., Rosenberger, A.E., Thurow, R.F., Dolloff, C.A., and Howell, P.J. 2009.
491 Coldwater fish in wadeable streams. Pages 119-138 in Bonar, S.A., Hubert, W.A., Willis,
492 D.W., editors. Standard methods for sampling North American freshwater fishes. American
493 Fisheries Society, Bethesda, Maryland.
- 494 Durance, I., Le Pichon, C., and Ormerod, S. J. 2006. Recognizing the importance of scale in the
495 ecology and management of riverine fish. Riv. Res. Appl. **22**(10):1143-1152. doi:
496 10.1002/rra.965.
- 497 Elith, J., and Leathwick, J.R., 2009. Species distribution models: ecological explanation and
498 prediction across space and time. Annual Review of Ecology, Evolution, and Systematics
499 **40**(1):677-697. doi: 10.1146/annurev.ecolsys.110308.120159.
- 500 Falke, J.A., Dunham, J.B., Jordan, C.E., McNyset, K.M., and Reeves, G.H. 2013. Spatial
501 ecological processes and local factors predict the distribution and abundance of spawning by
502 steelhead (*Oncorhynchus mykiss*) across a complex riverscape. PLoS ONE **8**(11): e79232.
503 doi: 10.1371/journal.pone.0079232.
- 504 Falk, M.G., McGree, J.M., and Pettitt, A.N. 2014. Sampling designs on stream networks using
505 the pseudo-Bayesian approach. Environ. Ecol. Statist. **21**(4):751-773. doi: 10.1007/s10651-
506 014-0279-2.
- 507 Fausch, K.D., Hawkes, C.L., and Parsons, M.G. 1988. Models that predict standing crop of
508 stream fish from habitat variables: 1950–85. Gen. Tech. Rep. PNW-GTR-213. Portland, OR:
509 U.S. Department of Agriculture, Forest Service, Pacific Northwest Research Station; 52
510 pages.

- 511 Fausch, K.D., Torgersen, C.E., Baxter, C.V., and Li, H.W. 2002. Landscapes to riverscapes:
512 Bridging the gap between research and conservation of stream fishes. *BioScience* **52**(6):483-
513 498. doi: 10.1641/0006-3568(2002)052[0483:LTRBTG]2.0.CO;2.
- 514 Franklin, I.R. 1980. Evolutionary change in small populations. Pages 135–149 In Soulé, M.E.,
515 and Wilcox, B.A. (Eds.). *Conservation Biology: An Evolutionary-Ecological Perspective*.
516 Sinauer, Sunderland, MA.
- 517 Frieden, J.C., Peterson, E.E., Webb, J.A., and Negus, P.M. 2014. Improving the predictive power
518 of spatial statistical models of stream macroinvertebrates using weighted autocovariance
519 functions. *Environ. Model. Soft.* **60**:320-330. doi:10.1016/j.envsoft.2014.06.019.
- 520 Fritz, K.M. Hagenbuch, E., D'Amico, E., Reif, M., Wigington, P.J. Jr., Leibowitz, S.G.,
521 Comeleo, R.L., Ebersole, J.L., and Nadeau, T. 2013. Comparing the extent and permanence
522 of headwater streams from two field surveys to values from hydrographic databases and
523 maps. *Journal of the American Water Resources Association* **49**(4): 867-882. doi:
524 10.1111/jawr.12040.
- 525 Ganio, L.M., Torgersen, C.E., and Gresswell, R.E. 2005. A geostatistical approach for describing
526 spatial pattern in stream networks. *Front. Ecol. Environ.* **3**(3):138-144. doi: 10.1890/1540-
527 9295(2005)003[0138:AGAFDS]2.0.CO;2.
- 528 Garreta, V., Monestiez, P. and Ver Hoef, J.M., 2010. Spatial modelling and prediction on river
529 networks: up model, down model or hybrid? *Environmetrics* **21**(5):439-456. doi:
530 10.1002/env.995.
- 531 Gelwicks, K.R., Zafft, D.J., and Gipson, R.G. 2002. Comprehensive study of the Salt River
532 fishery between Afton and Palisades Reservoir from 1995 to 1999 with historical review: fur
533 trade to 1998. Wyoming Game and Fish Department, Fish Division, Cheyenne.
- 534 Hankin, D.G., and Reeves, G.H. 1988. Estimating total fish abundance and total habitat area in
535 small streams based on visual estimation methods. *Can. J. Fish. Aq. Sci.* **45**(5):834–844. doi:
536 10.1139/f88-101.
- 537 Hanks, E.M., Schliep, E.M., Hooten, M.B. and Hoeting, J.A. 2015. Restricted spatial regression
538 in practice: geostatistical models, confounding, and robustness under model
539 misspecification. *Environmetrics* **26**(4):243-254. doi: 10.1002/env.2331.

- 540 Hawkins, C.P., Olsen, J.R., and Hill, R.A. 2010. The reference condition: predicting benchmarks
541 for ecological and water-quality assessments. *J. N. Am. Benthol. Soc.* **29**(1):312–343. doi:
542 10.1899/09-092.1.
- 543 Hilborn, R., and Walters, C.J. 1992. Quantitative fisheries stock assessment: choice, dynamics,
544 and uncertainty. Chapman and Hall, New York.
- 545 Hilderbrand, R.H., and Kershner, J.L. 2000. Conserving inland cutthroat trout in small streams:
546 how much stream is enough? *N. Am. J. Fish. Manage* **20**(2):513–520. doi: 10.1577/1548-
547 8675(2000)020<0513:CICTIS>2.3.CO;2.
- 548 Hill, R.A., Weber, M.H., Leibowitz, S.G., Olsen, A.R., and Thornbrugh, D.J. 2016. The stream-
549 catchment (StreamCat) dataset: A database of watershed metrics for the conterminous United
550 States. *J. Am. Wat. Res. Ass.* **52**(1):120-128. doi: 10.1111/1752-1688.12372.
- 551 Hodges J.S, and Reich B.J. 2010. Adding spatially-correlated errors can mess up the fixed effect
552 you love. *The American Statistician* **64**(4):325–334. doi: [10.1198/tast.2010.10052](https://doi.org/10.1198/tast.2010.10052).
- 553 Homer, C.G., Dewitz, J.A., Yang, L., Jin, S., Danielson, P., Xian, G., Coulston, J., Herold, N.D.,
554 Wickham, J.D. and Megown, K., 2015. Completion of the 2011 National Land Cover
555 Database for the conterminous United States-Representing a decade of land cover change
556 information. *Photogramm. Eng. Remote Sens.* **81**(5):345-354. doi: 10.14358/PERS.81.5.345.
- 557 Isaak, D.J., and Hubert, W.A. 2004. Nonlinear response of trout abundance to summer stream
558 temperatures across a thermally diverse montane landscape. *Trans. Am. Fish. Soc.*
559 **133**(5):1254–1259. doi: 10.1577/T03-010.1.
- 560 Isaak, D.J., Luce, C.H., Rieman, B.E., Nagel, D.E., Peterson, E.E., Horan, D.L., Parkes, S., and
561 Chandler, G.L. 2010. Effects of climate change and wildfire on stream temperatures and
562 salmonid thermal habitat in a mountain river network. *Ecol. Appl.* **20**(5):1350–1371. doi:
563 10.1890/09-0822.1.
- 564 Isaak, D.J., Wenger, S.J., Peterson, E.E., Ver Hoef, J.M., Hostetler, S., Luce, C.H., Dunham,
565 J.B., Kershner, J., Roper, B.B., Nagel, D.E., Chandler, G.L., Wollrab, S., Parkes, S., and
566 Horan, D.L. 2016. NorWeST modeled summer stream temperature scenarios for the western
567 U.S. U.S. Forest Service, Rocky Mountain Research Station Research Data Archive.
568 <https://doi.org/10.2737/RDS-2016-0033>.
- 569 Isaak, D.J., Peterson, E.E., Nagel, D.E., Ver Hoef, J.M., and Kershner, J. 2013. A national stream
570 internet to facilitate accurate, high-resolution status and trend assessments for water quality

- 571 parameters and aquatic biotas. U.S. Fish and Wildlife Service, National Landscape
572 Conservation Cooperative grant. Project website:
573 www.fs.fed.us/rm/boise/AWAE/projects/NationalStreamInternet.html.
- 574 Isaak, D.J., Peterson, E.E., Ver Hoef, J.M., Wenger, S., Falke, J., Torgersen, C., Sowder, C.,
575 Steel, A., Fortin, M., Jordan, C., Reusch, A., Som, N., and Monestiez, P. 2014. Applications
576 of spatial statistical network models to stream data. *WIREs -Water* **1**(3):277–294. doi:
577 10.1002/wat2.1023.
- 578 Isaak, D.J., Wenger, S., Young, M.K. 2017. Big biology meets microclimatology: Defining
579 thermal niches of aquatic ectotherms at landscape scales for conservation planning. *Ecol.*
580 *Appl.* doi:
- 581 Kershner, J.L., and Roper, B.B. 2010. An evaluation of management objectives used to assess
582 stream habitat conditions on federal lands within the interior Columbia Basin. *Fisheries*
583 **35**(6):269-278. doi: 10.1577/1548-8446-35.6.269
- 584 Korman, J., Schick, J., and Mossop, B. 2016. Estimating riverwide abundance of juvenile fish
585 populations: How much sampling is enough? *N. Am. J. Fish. Manage.* **36**(2):213-229. doi:
586 10.1080/02755947.2015.1114542.
- 587 Lincoln, F. C. 1930. Calculating waterfowl abundance on the basis of banding returns. United
588 States Department of Agriculture Circular **118**:1–4.
- 589 Loftus, A.J., and Beard, T.D. 2009. The multistate aquatic resources information system
590 (MARIS): Sharing data across agency boundaries. In: Bonar, S.A.; Hubert, W.A.; Willis,
591 D.W., eds. Standard methods for sampling North American freshwater fishes. Bethesda, MD:
592 American Fisheries Society: 187.
- 593 Matheron, G. 1963. Principles of geostatistics. *Econ. Geol.* **58**(8):1246–1266. doi:
594 10.2113/gsecongeo.58.8.1246.
- 595 McKay, L., Bondelid, T., Dewald, T., Johnston, J., Moore, R., and Rea, A. 2012. NHDPlus
596 Version 2: User Guide. [ftp://ftp.horizon-](ftp://ftp.horizon-systems.com/NHDPlus/NHDPlusV21/Documentation/NHDPlusV2_User_Guide.pdf)
597 [systems.com/NHDPlus/NHDPlusV21/Documentation/NHDPlusV2_User_Guide.pdf](ftp://ftp.horizon-systems.com/NHDPlus/NHDPlusV21/Documentation/NHDPlusV2_User_Guide.pdf)
- 598 Meyer, K.A., and High, B. 2011. Accuracy of removal electrofishing estimates of trout
599 abundance in Rocky Mountain streams. *N. Am. J. Fish. Manage.* **31**(5):923-933. doi:
600 10.1080/02755947.2011.633684.

- 601 Meyer, K.A., Lamansky, J.A., Schill, D.J., and Zaroban, D.W. 2013. Nongame fish species
602 distribution and habitat associations in the Snake River basin of southern Idaho. *Western*
603 *North American Naturalist* **73**(1):20-34. doi: 10.3398/064.073.0102.
- 604 Millar, C.P., Fryer, R.J., Millidine, K.J., Malcolm, I.A. 2016. Modelling capture probability of
605 Atlantic salmon (*Salmo salar*) from a diverse national electrofishing dataset: Implications for
606 the estimation of abundance. *Fisheries Research* **177**(1):1-12.
607 doi.org/10.1016/j.fishres.2016.01.001.
- 608 Moore, R.B., and Dewald, T.G. 2016. The road to NHDPlus—Advancements in digital stream
609 networks and associated catchments. *Journal of the American Water Resources Association*.
610 doi: 10.1111/1752-1688.12389.
- 611 Nagel, D.E., Buffington, J.M., Parkes, S.L., Wenger, S. and Goode, J.R. 2014. A landscape scale
612 valley confinement algorithm: delineating unconfined valley bottoms for geomorphic,
613 aquatic, and riparian applications. Gen. Tech. Rep. RMRS-GTR- 321. Fort Collins, CO: U.S.
614 Department of Agriculture, Forest Service, Rocky Mountain Research Station. 42 p.
- 615 Petersen, C.G. 1896. The yearly immigration of young plaice into the Limfjord from the German
616 Sea. *Report of the Danish Biological Station* **6**:5–84.
- 617 Peterson, J.T., Thurow, R.F., and Guzevich, J.W., 2004. An evaluation of multipass
618 electrofishing for estimating the abundance of stream-dwelling salmonids. *Trans. Am. Fish.*
619 *Soc.* **133**(2):462–475. doi: 10.1577/03-044.
- 620 Peterson, E.E., and Ver Hoef, J.M. 2010. A mixed-model moving-average approach to
621 geostatistical modeling in stream networks. *Ecology* **91**(3):644–651. doi: 10.1890/08-1668.1.
- 622 Peterson E.E, and Ver Hoef, J.M. 2014. STARS: an ArcGIS toolset used to calculate the spatial
623 information needed to fit spatial statistical models to stream network data. *J. Stat. Softw.*
624 **56**(2):1–17. doi: 10.18637/jss.v056.i02.
- 625 Peterson, E.E., Sheldon, F., Darnell, R., Bunn, S.E. and Harch, B.D., 2011. A comparison of
626 spatially explicit landscape representation methods and their relationship to stream condition.
627 *Freshwater Biology* **56**(3):590-610. doi: 10.1111/j.1365-2427.2010.02507.x.
- 628 Peterson, E.E., Ver Hoef, J.M., Isaak, D.J., Falke, J.A., Fortin, M.J., Jordan, C.E., McNyset, K.,
629 Monestiez, P., Ruesch, A.S., Sengupta, A. and Som, N., 2013. Modelling dendritic ecological
630 networks in space: an integrated network perspective. *Ecol. Lett.* **16**(5):707-719. doi:
631 10.1111/ele.12084.

- 632 Pollock, K.H., Nichols, J.D., Brownie, C., and Hines, J.E. 1990. Statistical inference for capture-
633 recapture experiments. *Wildlife Monographs*. No. 107.
- 634 R Development Core Team. 2014. R: A language and environment for statistical computing. R
635 Foundation for Statistical Computing, Vienna, Austria.
- 636 Rushworth, A.M., Peterson, E.E., Ver Hoef, J.M. and Bowman, A.W. 2015. Validation and
637 comparison of geostatistical and spline models for spatial-stream-networks. *Environmetrics*
638 **26**(5):327-338. doi: 10.1002/env.2340.
- 639 Schabenberger, O. and Gotway, C.A. 2005. *Statistical Methods for Spatial Data Analysis*.
640 Chapman and Hall/CRC, Boca Raton, FL.
- 641 Schlosser, I.J. 1991. Stream fish ecology: A landscape perspective. *BioScience* **41**(10):704–712.
642 doi: 10.2307/1311765.
- 643 Som, N.A., Monestiez, P., Ver Hoef, J.M., Zimmerman, D.L., and Peterson, E.E. 2014. Spatial
644 sampling on streams: Principles for inference on aquatic networks. *Environmetrics*
645 **25**(5):306-323. doi: 10.1002/env.2284.
- 646 Stevens, D.L., Jr., and Olsen, A.R. 2004. Spatially balanced sampling of natural resources. *J.*
647 *Am. Stat. Assoc.* **99**(465):262–278. doi: 10.1198/016214504000000250.
- 648 Temesgen, H., and Ver Hoef, J.M. 2015. Evaluation of the spatial linear model, random forest
649 and gradient nearest-neighbor methods for imputing potential productivity and biomass of
650 the Pacific Northwest forests. *Forestry* **88**(1):131-142. doi: 10.1093/forestry/cpu036.
- 651 Thompson, S. K. 1992. *Sampling*. John Wiley & Sons, New York, NY.
- 652 Thorson, J.T., Ianelli, J.N., Munch, S.B., Ono, K., and Spencer, P.D. 2015. Spatial delay-
653 difference models for estimating spatiotemporal variation in juvenile production and
654 population abundance. *Can. J. Fish. Aquat. Sci.* **72**(12): 1897–1915. doi:10.1139/cjfas-2014-
655 0543.
- 656 Torgersen C.E., Baxter C.V., Li, H.W., and McIntosh, B.A. 2006. Landscape influences on
657 longitudinal patterns of river fishes: spatially continuous analysis of fish-habitat
658 relationships. In: Hughes, R.M., Wang, L., and Seelbach, P.W. (eds) *Landscape Influences*
659 *on Stream Habitats and Biological Assemblages*, Vol. 48. Bethesda, MD: American Fisheries
660 Society, pp. 473–492.

- 661 Turschwell, M.P., Peterson, E.E., Balcombe, S.R., and Sheldon, F. 2016. To aggregate or not?
662 Capturing the spatio-temporal complexity of the thermal regime. *Ecol. Indicat.* **67**:39-48. doi:
663 10.1016/j.ecolind.2016.02.014.
- 664 Ver Hoef, J.M. 2002. Sampling and geostatistics for spatial data. *Ecoscience* **9**(2):152-161.
- 665 Ver Hoef, J.M. 2008. Spatial methods for plot-based sampling of wildlife populations. *Environ.*
666 *Ecol. Stat.* **15**(1):3-13. doi: 10.1007/s10651-007-0035-y.
- 667 Ver Hoef, J.M., and Peterson, E.E. 2010. A moving average approach for spatial statistical
668 models of stream networks. *J. Am. Stat. Assoc.* **105**(489):6–18. doi:
669 10.1198/jasa.2009.ap08248.
- 670 Ver Hoef, J.M., Peterson, E.E., and Theobald, D. 2006. Spatial statistical models that use flow
671 and stream distance. *Environ. Ecol. Stat.* **13**(4):449–464. doi: 10.1007/s10651-006-0022-8.
- 672 Ver Hoef, J.M., Peterson, E.E., Clifford, D., and Shah, R. 2014. SSN: An R package for spatial
673 statistical modeling on stream networks. *J. Stat. Softw.* **56**(3):1–45. doi:
674 10.18637/jss.v056.i03.
- 675 Wang, L., Infante, D., Esselman, P., Cooper, A., Wu, D., Taylor, W., Beard, D., Whelan, G., and
676 Ostroff, A. 2011. A hierarchical spatial framework and database for the national river fish
677 habitat condition assessment. *Fisheries* **36**(9):436-449. doi: 10.1080/03632415.2011.607075.
- 678 Webster, R.A., K.H. Pollock, S.K. Ghosh, and Hankin, D.G. 2008. Bayesian spatial modeling of
679 data from unit-count surveys of fish in streams. *Trans. Am. Fish. Soc.* **137**(2):438–453. doi:
680 10.1577/T06-138.1.
- 681 Wenger, S., Isaak, D.J., Luce, C., Neville, H., Fausch, K., Dunham, J., Dauwalter, D., Young,
682 M., Elsner, M., Rieman, B., Hamlet, A., and Williams, J. 2011. Flow regime, temperature,
683 and biotic interactions drive differential declines of Rocky Mountain trout species under
684 climate change. *Proc. Nat. Acad. Sci.* **108**(34):14175-14180. doi: 10.1073/pnas.1103097108.
- 685 Wyatt, R.J. 2003. Mapping the abundance of riverine fish populations: integrating hierarchical
686 Bayesian models with a geographic information system (GIS). *Can. J. Fish. Aquat. Sci.*
687 **60**(8): 997–1006. doi: 10.1139/f03-085
- 688 Zale, A.V., Parrish, D.L., and Sutton, T.M. 2013. *Fisheries techniques*, third edition. American
689 Fisheries Society, Bethesda, MD. 1,009 pages.

- 690 Zimmerman, D., and Ver Hoef, J. M. 2017. The Torgegram for fluvial variography:
691 characterizing spatial dependence on stream networks. *J. Computational Graphical Stat.* doi:
692 10.1080/10618600.2016.1247006
- 693 Zippin, C. 1958. The removal method of population estimation. *J. Wild. Manage.* **22**(1):82–90.
694 doi: 10.2307/3797301.

Draft

695 **Table 1.** Summary statistics for trout densities and geospatial representations of habitat characteristics at 108 reaches across the Salt
 696 River network.

Variable	Mean	Median	SD	Minimum	Maximum	Data source
Trout•100 m ⁻¹	32.6	25.0	29.4	0	132	Gelwicks et al. (2002); Isaak and Hubert (2004)
August mean stream temperature (°C)	11.1	11.5	2.42	5.06	15.6	NorWeST (www.fs.fed.us/rm/boise/AWAE/projects/NorWeST.html ; Isaak et al. 2016)
Reach slope (%)	3.00	2.70	2.60	0.015	10.0	NHDPlus Value Added Attribute (www.horizon-systems.com/NHDPlus/index.php ; McKay et al. 2012)
Canopy (%)	30.7	31.9	16.9	0	80.1	National Land Cover Dataset (www.mrlc.gov/nlcd2001.php ; Homer et al. 2015)

697

698 **Table 2.** Summary statistics for multiple linear regression (MLR) and spatial-stream-network (SSN) models fit to trout density data at
 699 108 sites in the Salt River network.

Model	Covariates	<i>b</i> (SE)	p-value	Autocovariance	<i>p</i> [*]	ΔAIC	CV <i>r</i> ²⁺	RMSPE [‡]
MLR	Intercept	-55.0 (20.5)	< 0.01	--	4	27	0.19	26.3
	Slope	36.7 (126)	0.77					
	Temperature	6.75 (1.43)	< 0.01					
	Canopy	0.379 (0.163)	0.02					
SSN1	Intercept	-51.6 (29.1)	0.08	TU, TD	9	1	0.49	21.0
	Slope	103 (103)	0.32					
	Temperature	6.61 (2.22)	< 0.01					
	Canopy	0.255 (0.173)	0.14					
SSN2	Intercept	-51.4 (29.7)	0.09	TU, TD, EUC	11	5	0.49	20.9
	Slope	104 (104)	0.32					
	Temperature	6.60 (2.27)	< 0.01					
	Canopy	0.249 (0.18)	0.16					
SSN3	Intercept	-18.3 (19.1)	0.34	TU, TD	7	0	0.49	20.8
	Temperature	4.57 (1.67)	< 0.01					
SSN4	Intercept	31.9 (5.69)	< 0.01	TU, TD	6	5	0.49	20.9
SSN5	Intercept	31.4 (9.00)	< 0.01	TU, TD, EUC	8	7	0.50	20.5

700 ^{*}Number of model parameters. In addition to covariate parameters, SSN models include 3–7 parameters associated with the
 701 autocovariance construction (Ver Hoef and Peterson 2010).

702 [†]Squared correlation between the leave-one-out cross-validation prediction and observed trout densities.

703 [‡]Root mean square prediction error.

704 **Fig. 1.** Salt River watershed in the western U.S. and locations of trout density estimates at 108
705 sites. Population estimates were subsequently made for areas upstream of the green bars on
706 tributaries and downstream of the green bar on the Salt River mainstem.

707

708 **Fig. 2.** Empirical Torgegram describing patterns in spatial similarity among trout densities at 108
709 sites. Symbol sizes are proportional to the number of data pairs averaged for each semivariance
710 value.

711

712 **Fig. 3.** Comparison of leave-one-out cross validation (LOOCV) predictions for trout density
713 derived from a multiple linear regression (A) and a spatial-stream-network model (SSN3, B).
714 Dashed line indicates 1:1 relationship.

715

716 **Fig. 4.** Trout density map predicted by universal kriging and a spatial-stream-network model
717 (SSN3) fit to 108 samples. Stream lines are colored by predicted values and the width of the
718 black stream border is proportional to prediction standard errors. Population estimates were
719 made for areas upstream of the green bars on tributaries and downstream of the green bar on the
720 Salt River mainstem. Predictions were not made in the downstream extents of several eastern
721 tributaries and an upper section of the Salt River where channels are dewatered during the
722 summer.

723

724 **Fig. 5.** Trout population estimates for four tributary streams derived from simple random sample
725 (SRS) and spatial-stream-network (SSN) block-kriging estimators. Error bars denote 95%
726 confidence intervals; sample sizes are the number of fish density surveys conducted within each
727 tributary. A SRS estimate was not possible for Swift Creek where a single site was sampled.

728

729 **Fig. 6.** Trout population estimates from simple random sample (SRS) and spatial-stream-network
730 (SSN3) block-kriging estimators for the Salt River mainstem and tributary streams draining the
731 western (A) and eastern (B) sides of the watershed. Error bars denote 95% confidence intervals;
732 SRS estimates were not possible for Strawberry Creek and Swift Creek where single sites were
733 sampled.

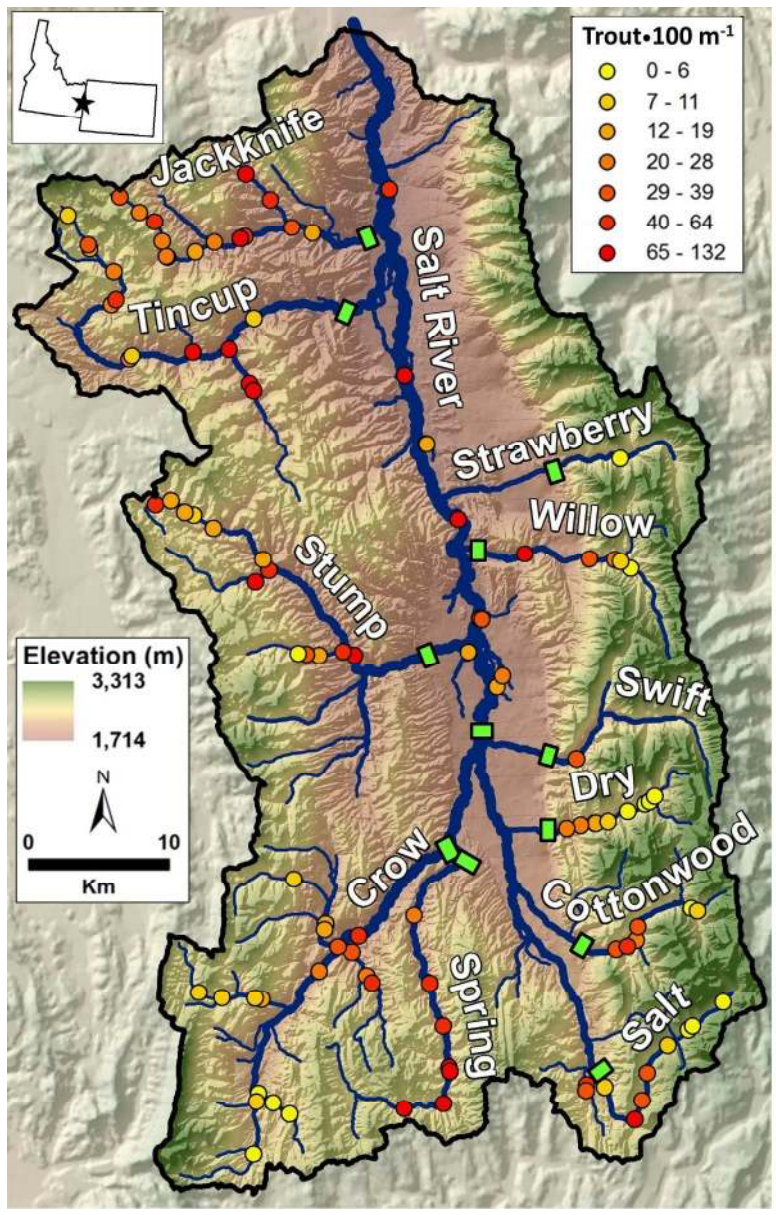


Figure 1.

fig 1

190x254mm (300 x 300 DPI)

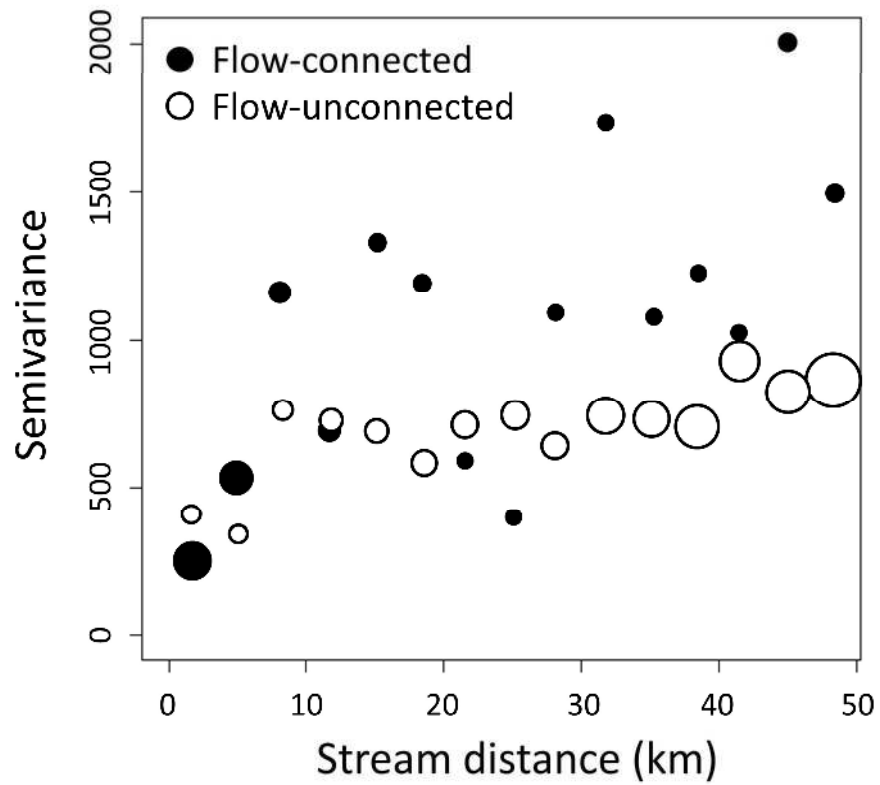
**Figure 2.**

Fig 2

190x254mm (300 x 300 DPI)

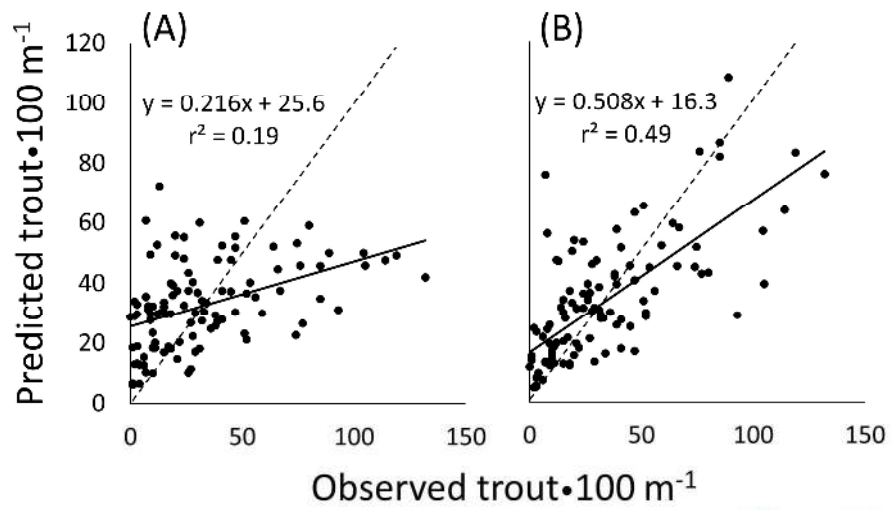
**Figure 3.**

Fig 3

190x254mm (300 x 300 DPI)

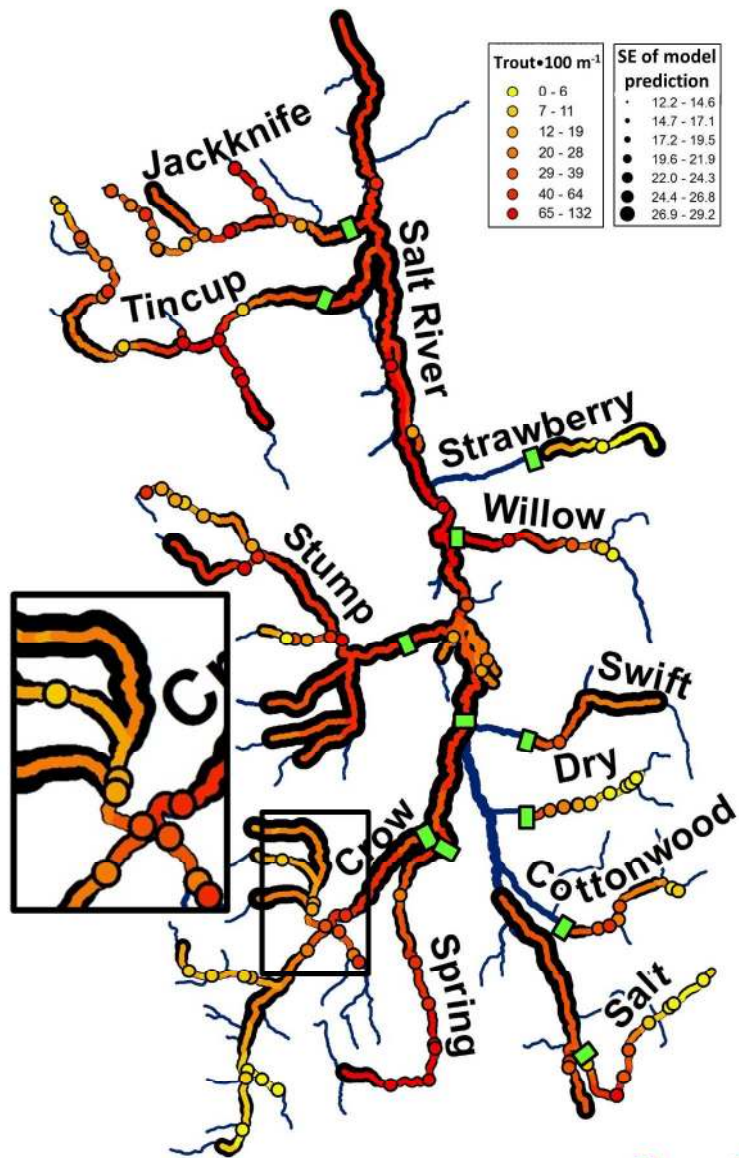


Figure 4.

fig 4

190x254mm (300 x 300 DPI)

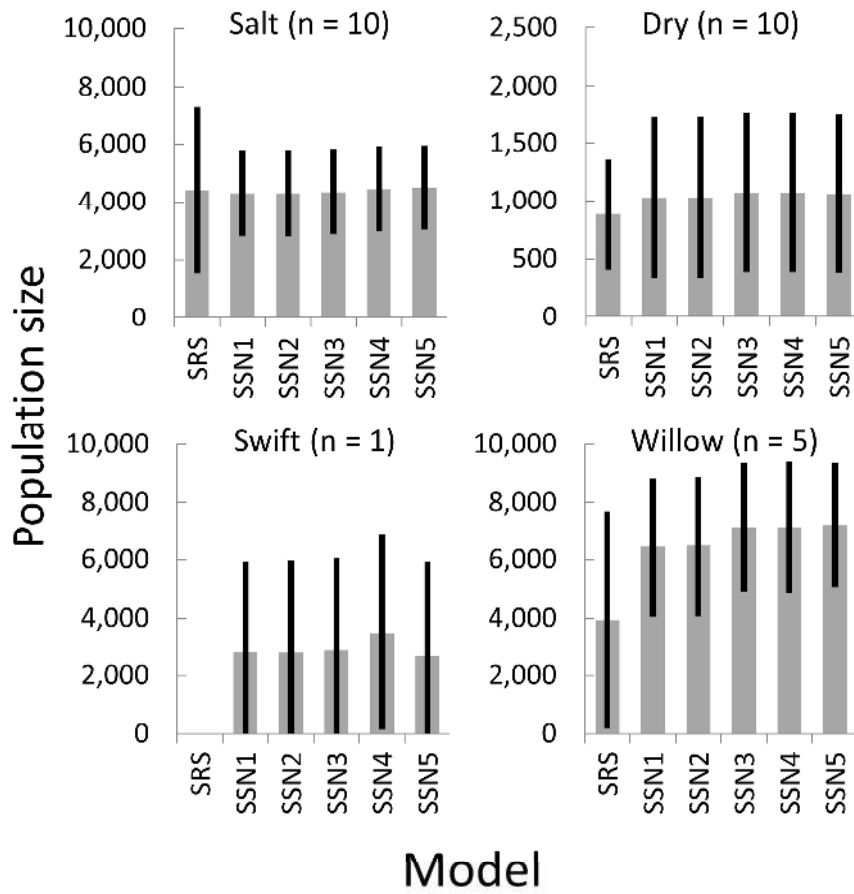


Figure 5.

fig 5

190x254mm (300 x 300 DPI)

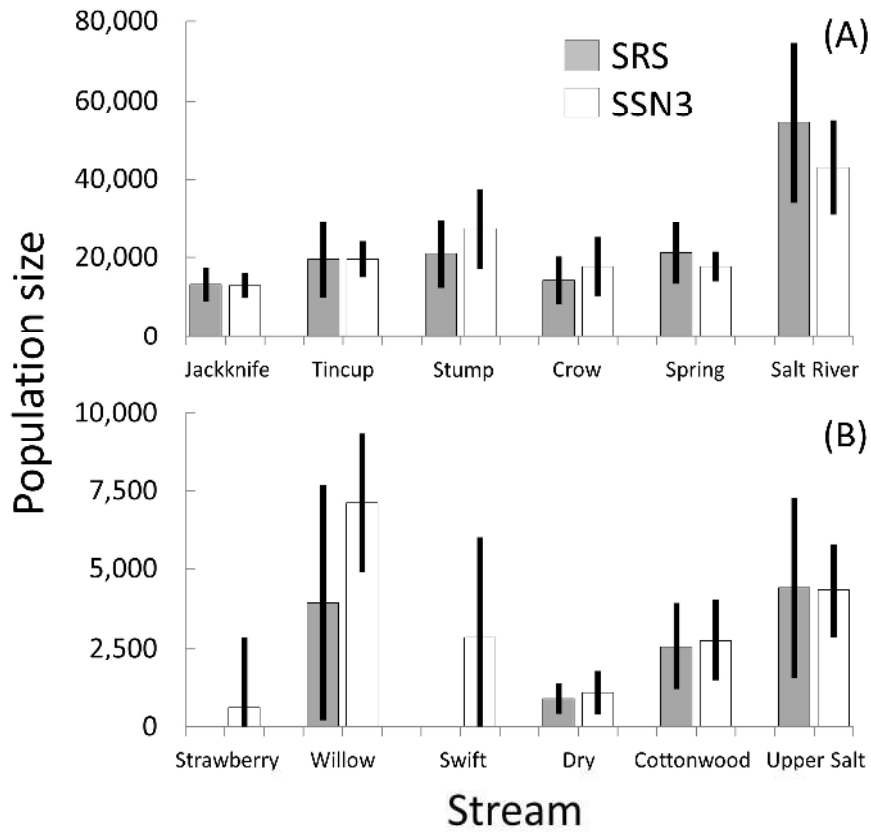


Figure 6.

fig 6

190x254mm (300 x 300 DPI)

Supplemental A. ZIP file containing the LSN object file “LSN_TroutDensity_BlockKrige.ssn” and ESRI geodatabase “LSN_TroutDensity_BlockKrige.mdb” to replicate the Salt River analysis is downloadable at the SSN/STARS website “Software and Data” subpage (www.fs.fed.us/rm/boise/AWAE/projects/SSN_STARS/software_data.html).

Supplemental B. Annotated R script “SaltRiver_TroutDensity_BlockKriging.R” used to model trout densities in the Salt River and derive block-kriging population estimates with the LSN object file from Appendix 1.

```
#Load SSN package into R
library("SSN")

#Set working directory to location of .ssn directory
setwd("C:\\...")

#import the data from the .ssn directory and create a SpatialStreamNetwork object with basic set
of prediction points for all reach midpoints
SaltWQ <- importSSN("lsndata/LSN_TroutDensity_BlockKrige.ssn", predpts = "preds")

#Import prediction points spaced at 100m intervals for block-kriging estimates of individual
streams
SaltWQ <- importPredpts(SaltWQ, "Cottonwood", "ssn")
SaltWQ <- importPredpts(SaltWQ, "Crow", "ssn")
SaltWQ <- importPredpts(SaltWQ, "Dry", "ssn")
SaltWQ <- importPredpts(SaltWQ, "Jackknife", "ssn")
SaltWQ <- importPredpts(SaltWQ, "Salt", "ssn")
SaltWQ <- importPredpts(SaltWQ, "Spring", "ssn")
SaltWQ <- importPredpts(SaltWQ, "Strawberry", "ssn")
SaltWQ <- importPredpts(SaltWQ, "Stump", "ssn")
SaltWQ <- importPredpts(SaltWQ, "Swift", "ssn")
SaltWQ <- importPredpts(SaltWQ, "Tincup", "ssn")
SaltWQ <- importPredpts(SaltWQ, "Willow", "ssn")
SaltWQ <- importPredpts(SaltWQ, "SaltRiver", "ssn")

#Import prediction points spaced at 100m intervals for block-kriging estimate of full network
SaltWQ <- importPredpts(SaltWQ, "Network", "ssn")

#Create distance matrices among stream prediction points
createDistMat(SaltWQ, predpts = "preds", o.write = TRUE, amongpreds = TRUE)
createDistMat(SaltWQ, predpts = "Cottonwood", o.write = TRUE, amongpreds = TRUE)
createDistMat(SaltWQ, predpts = "Crow", o.write = TRUE, amongpreds = TRUE)
createDistMat(SaltWQ, predpts = "Dry", o.write = TRUE, amongpreds = TRUE)
```

```

createDistMat(SaltWQ, predpts = "Jackknife", o.write = TRUE, amongpreds = TRUE)
createDistMat(SaltWQ, predpts = "Salt", o.write = TRUE, amongpreds = TRUE)
createDistMat(SaltWQ, predpts = "Spring", o.write = TRUE, amongpreds = TRUE)
createDistMat(SaltWQ, predpts = "Strawberry", o.write = TRUE, amongpreds = TRUE)
createDistMat(SaltWQ, predpts = "Stump", o.write = TRUE, amongpreds = TRUE)
createDistMat(SaltWQ, predpts = "Swift", o.write = TRUE, amongpreds = TRUE)
createDistMat(SaltWQ, predpts = "Tincup", o.write = TRUE, amongpreds = TRUE)
createDistMat(SaltWQ, predpts = "Willow", o.write = TRUE, amongpreds = TRUE)
createDistMat(SaltWQ, predpts = "SaltRiver", o.write = TRUE, amongpreds = TRUE)

#Create distance matrix among network prediction points (calculations require a few minutes)
createDistMat(SaltWQ, predpts = "Network", o.write = TRUE, amongpreds = TRUE)

#Describe the names of the variables in the point.data data.frame for each observed and
prediction data set
names(SaltWQ)

#plot Salt River network and locations of 108 trout density observations
plot(SaltWQ, lwdLineCol = "afvArea", lwdLineEx = 5, lineCol = "blue",
     pch = 19, xlab = "x-coordinate (m)", ylab = "y-coordinate (m)", asp = 1)

#plot values of 108 trout density observations (Figure 1)
brks <- plot(SaltWQ, "trout_100m", lwdLineCol = "afvArea",
            lwdLineEx = 5, lineCol = "black", xlab = "x-coordinate",
            ylab = "y-coordinate", asp=1 )

#plot Torgegram based on 108 trout density observations (Figure 2)
SaltWQ.Torg <- Torgegram(SaltWQ, "trout_100m", nlag = 15, nlagcutoff = 1, maxlag = 50000)
plot(SaltWQ.Torg)

#Fit nonspatial multiple linear regression (MLR) in Table 2
SaltWQ.glmssn0 <- glmssn(trout_100m ~ SLOPE + S1_93_11 + CANOPY, SaltWQ,
                        CorModels = NULL, use.nugget = TRUE, EstMeth = "REML")
summary(SaltWQ.glmssn0)

#Fit SSN1 in Table 2.
SaltWQ.glmssn1 <- glmssn(trout_100m ~ SLOPE + S1_93_11 + CANOPY, SaltWQ,
                        CorModels = c("Exponential.tailup", "Exponential.tailldown"),
                        addfunccol = "afvArea", EstMeth = "REML")
summary(SaltWQ.glmssn1)

#Fit SSN2 in Table 2.
SaltWQ.glmssn2 <- glmssn(trout_100m ~ SLOPE + S1_93_11 + CANOPY, SaltWQ,
                        CorModels = c("Exponential.tailup", "Exponential.tailldown", "Exponential.Euclid"),
                        addfunccol = "afvArea", EstMeth = "REML")
summary(SaltWQ.glmssn2)

```

#Fit SSN3 in Table 2.

```
SaltWQ.glmsn3 <- glmssn(trout_100m ~ S1_93_11, SaltWQ,
  CorModels = c("Exponential.tailup", "Exponential.taildown"),
  addfunccol = "afvArea", EstMeth = "REML")
summary(SaltWQ.glmsn3)
```

#Fit SSN4 in Table 2.

```
SaltWQ.glmsn4 <- glmssn(trout_100m ~ 1, SaltWQ,
  CorModels = c("Exponential.tailup", "Exponential.taildown"),
  addfunccol = "afvArea", EstMeth = "REML")
summary(SaltWQ.glmsn4)
```

#Fit SSN5 in Table 2.

```
SaltWQ.glmsn5 <- glmssn(trout_100m ~ 1, SaltWQ,
  CorModels = c("Exponential.tailup", "Exponential.taildown", "Exponential.Euclid"),
  addfunccol = "afvArea", EstMeth = "REML")
summary(SaltWQ.glmsn5)
```

#Report AIC values (Use ML instead of REML in above model fits to estimate correct AIC values)

```
AIC(SaltWQ.glmsn0)
AIC(SaltWQ.glmsn1)
AIC(SaltWQ.glmsn2)
AIC(SaltWQ.glmsn3)
AIC(SaltWQ.glmsn4)
AIC(SaltWQ.glmsn5)
```

#Report cross-validation statistics and confidence intervals

```
CrossValidationStatsSSN(SaltWQ.glmsn0)
CrossValidationStatsSSN(SaltWQ.glmsn1)
CrossValidationStatsSSN(SaltWQ.glmsn2)
CrossValidationStatsSSN(SaltWQ.glmsn3)
CrossValidationStatsSSN(SaltWQ.glmsn4)
CrossValidationStatsSSN(SaltWQ.glmsn5)
```

#Report variance composition among covariate effects and autocovariance functions

```
varcomp(SaltWQ.glmsn0)
varcomp(SaltWQ.glmsn1)
varcomp(SaltWQ.glmsn2)
varcomp(SaltWQ.glmsn3)
varcomp(SaltWQ.glmsn4)
varcomp(SaltWQ.glmsn5)
```

#Plot graphs of leave-one-out cross-validation (LOOCV) predictions & SEs

```
cv.out <- CrossValidationSSN(SaltWQ.glmsn2)
```

```

par(mfrow = c(1, 1))
plot(SaltWQ.glmssn2$sampinfo$z,
     cv.out[, "cv.pred"], pch = 19,
     xlab = "Observed Data", ylab = "LOOCV Prediction")

#Save LOOCV predictions & SEs to working directory file
write.csv(cv.out, "cv_out_trout100m.csv", row.names = FALSE)

#Calculate & plot model residuals & influence measures
resids <- residuals(SaltWQ.glmssn2)
class(resids)
resids.df <- getSSNdata.frame(resids)
names(resids.df)
plot(resids)
hist(resids, xlab = "Raw Residuals")
qqnorm(resids)

#Save residuals & influence measures to working directory file
write.csv(resids.df, "resids_trout100m.csv", row.names = FALSE)

#Plot 108 observation sites as large circles prior to block-kriging prediction points
plot(SaltWQ, "trout_100m", pch = 1, cex = 3,
     xlab = "x-coordinate (m)", ylab = "y-coordinate (m)",
     xlim = c(1715000,1770000), ylim = c(1370000,1450000))

#Plot 100m prediction points for individual stream blocks
SaltWQ.glmssn2.cottonwood <- predict(SaltWQ.glmssn2, "Cottonwood")
plot(SaltWQ.glmssn2.cottonwood, "trout_100m", add = TRUE,
     xlim = c(1715000,1770000), ylim = c(1370000,1450000))
SaltWQ.glmssn2.crow <- predict(SaltWQ.glmssn2, "Crow")
plot(SaltWQ.glmssn2.crow, "trout_100m", add = TRUE,
     xlim = c(1715000,1770000), ylim = c(1370000,1450000))
SaltWQ.glmssn2.dry <- predict(SaltWQ.glmssn2, "Dry")
plot(SaltWQ.glmssn2.dry, "trout_100m", add = TRUE,
     xlim = c(1715000,1770000), ylim = c(1370000,1450000))
SaltWQ.glmssn2.jackknife <- predict(SaltWQ.glmssn2, "Jackknife")
plot(SaltWQ.glmssn2.jackknife, "trout_100m", add = TRUE,
     xlim = c(1715000,1770000), ylim = c(1370000,1450000))
SaltWQ.glmssn2.salt <- predict(SaltWQ.glmssn2, "Salt")
plot(SaltWQ.glmssn2.salt, "trout_100m", add = TRUE,
     xlim = c(1715000,1770000), ylim = c(1370000,1450000))
SaltWQ.glmssn2.spring <- predict(SaltWQ.glmssn2, "Spring")
plot(SaltWQ.glmssn2.spring, "trout_100m", add = TRUE,
     xlim = c(1715000,1770000), ylim = c(1370000,1450000))
SaltWQ.glmssn2.strawberry <- predict(SaltWQ.glmssn2, "Strawberry")
plot(SaltWQ.glmssn2.strawberry, "trout_100m", add = TRUE,

```

```

xlim = c(1715000,1770000), ylim = c(1370000,1450000))
SaltWQ.glmsn2.stump <- predict(SaltWQ.glmsn2, "Stump")
plot(SaltWQ.glmsn2.stump, "trout_100m", add = TRUE,
     xlim = c(1715000,1770000), ylim = c(1370000,1450000))
SaltWQ.glmsn2.swift <- predict(SaltWQ.glmsn2, "Swift")
plot(SaltWQ.glmsn2.swift, "trout_100m", add = TRUE,
     xlim = c(1715000,1770000), ylim = c(1370000,1450000))
SaltWQ.glmsn2.tincup <- predict(SaltWQ.glmsn2, "Tincup")
plot(SaltWQ.glmsn2.tincup, "trout_100m", add = TRUE,
     xlim = c(1715000,1770000), ylim = c(1370000,1450000))
SaltWQ.glmsn2.willow <- predict(SaltWQ.glmsn2, "Willow")
plot(SaltWQ.glmsn2.willow, "trout_100m", add = TRUE,
     xlim = c(1715000,1770000), ylim = c(1370000,1450000))
SaltWQ.glmsn2.saltriver <- predict(SaltWQ.glmsn2, "SaltRiver")
plot(SaltWQ.glmsn2.saltriver, "trout_100m", add = TRUE,
     xlim = c(1715000,1770000), ylim = c(1370000,1450000))

#Obtain block-kriging estimates of mean trout density & SEs for individual stream blocks
SaltWQ.glmsn2.cottonwood <- BlockPredict(SaltWQ.glmsn2, "Cottonwood")
SaltWQ.glmsn2.cottonwood
SaltWQ.glmsn2.crow <- BlockPredict(SaltWQ.glmsn2, "Crow")
SaltWQ.glmsn2.crow
SaltWQ.glmsn2.dry <- BlockPredict(SaltWQ.glmsn2, "Dry")
SaltWQ.glmsn2.dry
SaltWQ.glmsn2.jackknife <- BlockPredict(SaltWQ.glmsn2, "Jackknife")
SaltWQ.glmsn2.jackknife
SaltWQ.glmsn2.salt <- BlockPredict(SaltWQ.glmsn2, "Salt")
SaltWQ.glmsn2.salt
SaltWQ.glmsn2.spring <- BlockPredict(SaltWQ.glmsn2, "Spring")
SaltWQ.glmsn2.spring
SaltWQ.glmsn2.strawberry <- BlockPredict(SaltWQ.glmsn2, "Strawberry")
SaltWQ.glmsn2.strawberry
SaltWQ.glmsn2.stump <- BlockPredict(SaltWQ.glmsn2, "Stump")
SaltWQ.glmsn2.stump
SaltWQ.glmsn2.swift <- BlockPredict(SaltWQ.glmsn2, "Swift")
SaltWQ.glmsn2.swift
SaltWQ.glmsn2.tincup <- BlockPredict(SaltWQ.glmsn2, "Tincup")
SaltWQ.glmsn2.tincup
SaltWQ.glmsn2.willow <- BlockPredict(SaltWQ.glmsn2, "Willow")
SaltWQ.glmsn2.willow
SaltWQ.glmsn2.SaltRiver <- BlockPredict(SaltWQ.glmsn2, "SaltRiver")
SaltWQ.glmsn2.SaltRiver

#Save values of block predictions & SEs at 100m prediction points to working directory file
SaltWQ.cottonwood <- predict(SaltWQ.glmsn2, "Cottonwood")
pred1df <- getSSNdata.frame(SaltWQ.cottonwood, "Cottonwood")

```



```
write.csv(pred1df, "SaltWQ_trout100m_SSN2_cottonwood_BlockPredictions.csv", row.names = FALSE)
```

```
#Plot 100m prediction points for full network  
SaltWQ.glmssn2.network <- predict(SaltWQ.glmssn2, "Network")  
plot(SaltWQ.glmssn2.network, "trout_100m", add = TRUE,  
      xlim = c(1715000,1770000), ylim = c(1370000,1450000))
```

```
#Obtain block-kriging estimates of mean trout density & SEs for full network (calculation requires several minutes)
```

```
SaltWQ.glmssn2.network <- BlockPredict(SaltWQ.glmssn2, "Network")  
SaltWQ.glmssn2.network
```

```
#Plot predictions for full network at reach midpoints with symbol size inverse to SEs
```

```
SaltWQ.preds <- predict(SaltWQ.glmssn2, "preds")  
plot(SaltWQ.preds, SEcex.max = 1.4, SEcex.min = .7/3*2,  
      breaktype = "user", brks = brks)
```

```
#Is this cool or what?
```

Draft